INTERNATIONAL ATOMIC ENERGY AGENCY
UNITED NATIONS EDUCATIONAL, SCIENTIFIC AND CULTURAL ORGANIZATION
INTERNATIONAL CENTRE FOR THEORETICAL PHYSICS
I.C.T.P., P.O. BOX 586, 34100 TRIESTE, ITALY, CABLE: CENTRATOM TRIESTE

SMR/384 - 3

EXPERIMENTAL WORKSHOP ON
"HIGH TEMPERATURE SUPERCONDUCTORS"
(30 March - 14 April 1989)

STRUCTURE INVESTIGATIONS

Lucio RANDACCIO
Dipartimento di Scienze Chimiche
Universita' degli Studi di Trieste
Piazzale Europa, 1
34100 Trieste
Italy

These are preliminary lecture notes, intended only for distribution to participants.

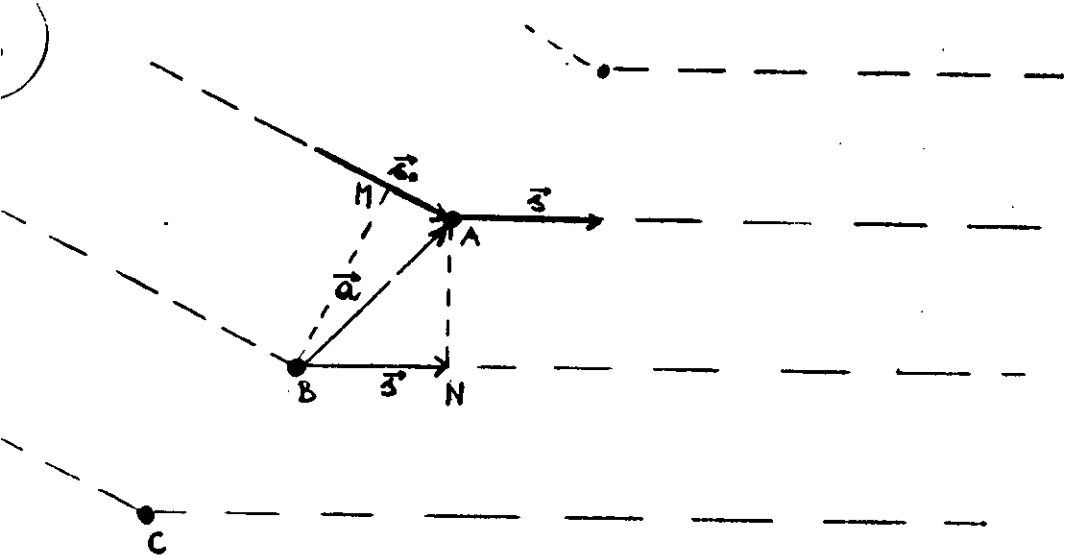

Q

$$|\vec{S}| = |\vec{S}_0| = \frac{1}{\lambda}$$

$$\Delta = \overline{BN} - \overline{AH} = \vec{a}(\vec{s} - \vec{s}_0)$$

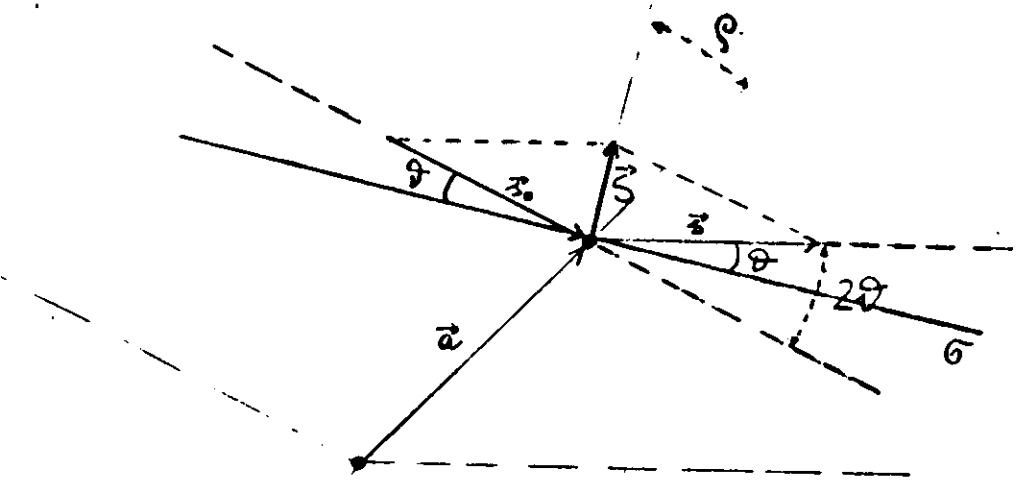

$$\Delta = \vec{a} \cdot \vec{S}$$

$$|\vec{S}| = \frac{2\sin\vartheta}{\lambda}$$

Line of identical scattering points

$$A_A = \frac{A^\circ}{R} e^{i\omega t}$$

$$A_B = \frac{A^\circ}{R} e^{i\omega t + 2\pi \vec{a}\cdot\vec{S}}$$

$$\vdots$$

$$A = \frac{A^\circ}{R} e^{i\omega t} \sum_{u=0}^{N_1-1} e^{i 2\pi u (\vec{a}\cdot\vec{S})}$$

$$I = A\cdot A^* = \frac{|A^\circ|^2}{R^2} \frac{\sin^2(N_1\psi_1)}{\sin^2\psi_1} \quad \text{where } \psi_1 = \tfrac{1}{2}\pi(\vec{a}\cdot\vec{S})$$

$$\text{if } N_1 \longrightarrow \infty$$

$$I_h = \frac{|A^\circ|^2}{R^2} N_1^2 \quad \text{when } \pi(\vec{a}\cdot\vec{S}) = h\pi \quad \text{with } h \text{ integer}$$

$$\vec{S}\cdot\vec{a} = h$$

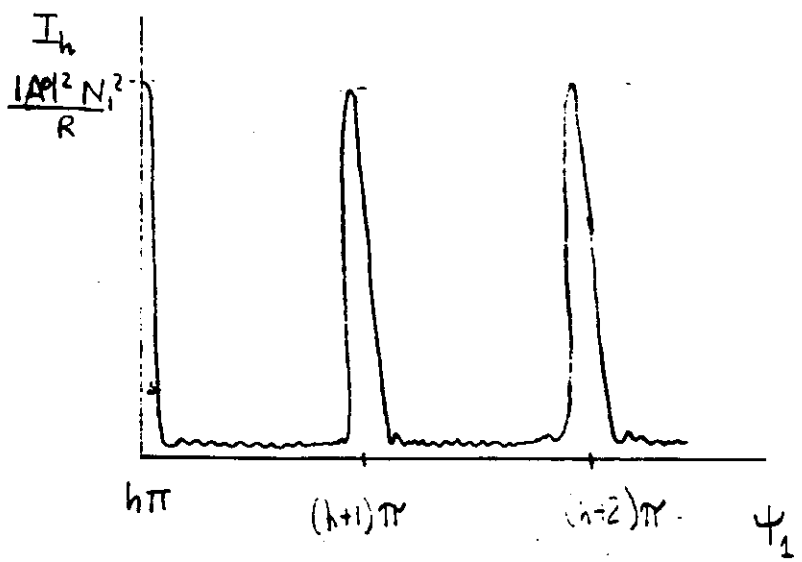

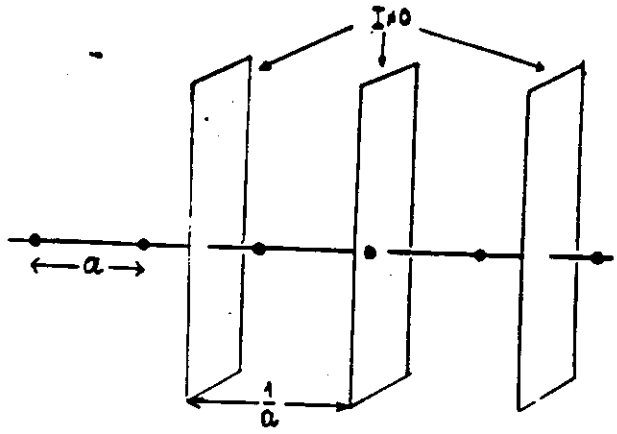

$\vec{S}\cdot\vec{a} = h$

$\vec{S}\cdot\vec{a} = h$
$\vec{S}\cdot\vec{b} = k$

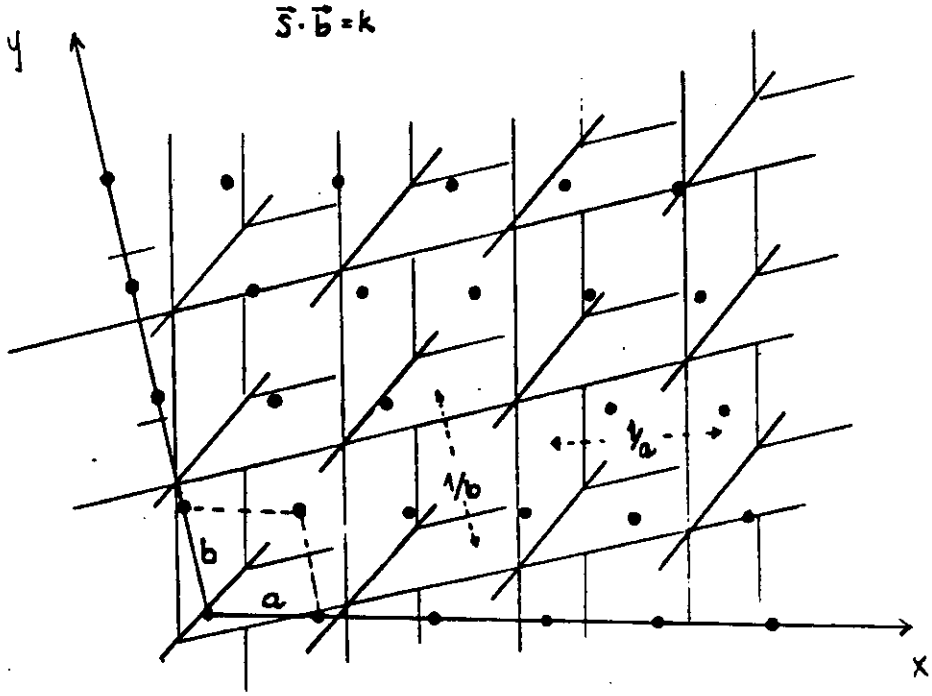

Space-lattice of identical scattering points

$$A = \frac{A^0}{R} e^{i\omega t} \sum_{u}^{N_1-1} \sum_{v}^{N_2-1} \sum_{w}^{N_3-1} e^{i2\pi(u\vec{a} + v\vec{b} + w\vec{c})\cdot\vec{S}}$$

$$I_{hkl} = \frac{|A^0|^2}{R^2} N_1^2 N_2^2 N_3^2 \qquad (N_1, N_2, N_3 \longrightarrow \infty)$$

$$\begin{aligned} \vec{S}\cdot\vec{a} &= h \\ \vec{S}\cdot\vec{b} &= k \\ \vec{S}\cdot\vec{c} &= l \end{aligned} \qquad (h, k, l \text{ integer})$$

Laue equations

$$\vec{S}\cdot\vec{a} = h \quad ; \quad 2\sin\vartheta \cdot a \cdot \cos\rho = h\lambda$$
$$\vec{S}\cdot\vec{b} = k \quad ; \quad 2\sin\vartheta \cdot b \cdot \cos\sigma = k\lambda \qquad (1) \qquad h,k,l \text{ integer}$$
$$\vec{S}\cdot\vec{c} = l \quad ; \quad 2\sin\vartheta \cdot c \cdot \cos\varphi = l\lambda$$

$$d_{hkl} = \frac{a}{h}\cos\rho = \frac{b}{k}\cos\sigma = \frac{c}{l}\cos\varphi \qquad (2)$$

Bragg equation $\underline{2\, d_{hkl} \sin\vartheta = \lambda}$; $\vec{OP} \equiv \vec{S}$

$$d_{hkl} = \frac{1}{|\vec{S}|_{hkl}}$$

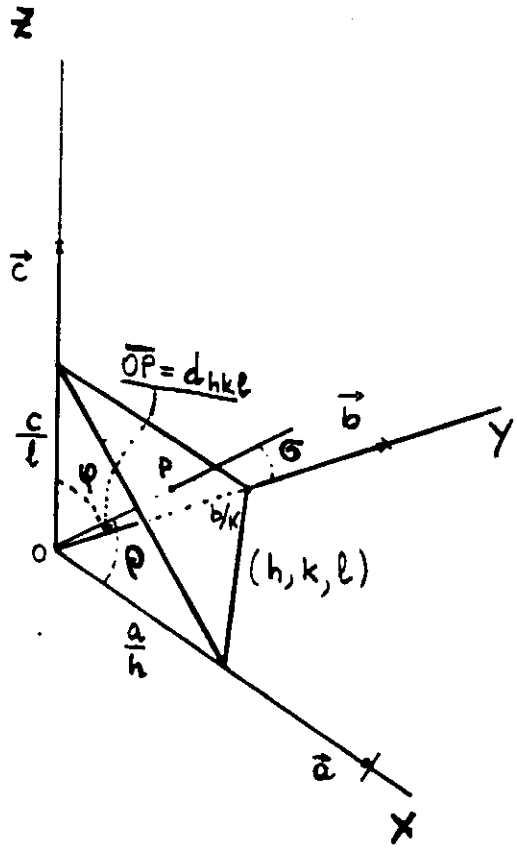

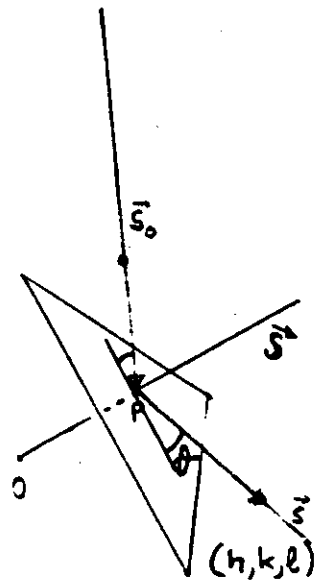

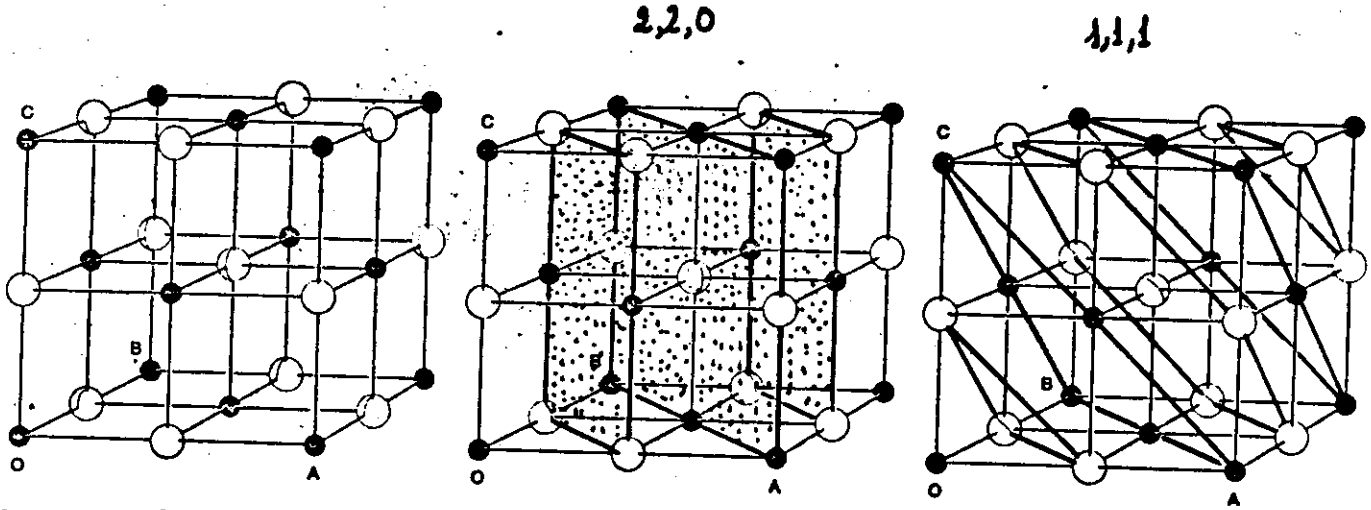

Questa figura mostra tre possibili disposizioni degli strati di atomi riflettenti in un cristallo di cloruro di sodio (*rappresentate mediante piani colorati*). Gli assi di questo semplice cristallo cubico sono indicati con *OA*, *OB* e *OC*. Nello schema a sinistra viene assegnato alla prima riflessione da parte di piani perpendicolari all'asse *OA* l'ordine (200), poiché vi è una differenza di percorso di due lunghezze d'onda tra *O* e *A* per piani riflettenti paralleli agli assi *OB* e *OC*; (in questo caso $h = 2$, $k = 0$ e $l = 0$). In modo analogo la riflessione iniziale da parte dei piani mostrati nello schema centrale viene designata con (220), mentre per lo schema a destra è (111) rispetto ai piani di cloro. In genere gli ordini con indici pari si riferiscono a strati identici, e hanno perciò come risultato riflessioni intense e in fase, mentre gli ordini con indici dispari provengono da strati occupati in modo alterno, e hanno perciò come risultato riflessioni deboli e sfasate.

Faremo qui un'analisi abbastanza dettagliata poiché, pur essendo questo particolare caso estremamente semplice, può esemplificare il procedimento generale. Uno sguardo ai diagrammi di struttura del cloruro di sodio mostra come i piani rappresentati siano di due tipi. Le riflessioni, o ordini, indicate con (200), (400), (600) ecc. e quelle indicate con (220), (440), (660) e così via hanno origine da strati atomici identici, ciascuno dei quali contiene un numero uguale di atomi di sodio e di cloro. Ci si aspetterebbe che la sequenza degli ordini successivi diminuisca regolarmente come intensità. Come mostra il disegno a destra della figura in alto, le riflessioni (111) provengono invece da un insieme di piani più complessi, in quanto gli strati sono alternativamente occupati da atomi di sodio e di cloro. Poiché per le riflessioni (111) vi è una differenza di percorso di una lunghezza d'onda rispetto ai piani intensamente riflettenti formati dagli atomi di cloro, le onde riflesse dai piani intermedi formati dagli atomi di sodio più debolmente riflettenti avranno fase opposta. L'ordine (111) sarà perciò debole, poiché il contributo del sodio annulla in parte quello del cloro; per l'ordine (222), invece, i contributi saranno in fase e quest'ordine sarà intenso.

In questo tipo di « reticolo spaziale », come viene chiamato, vi sono punti identici nel centro delle facce e nei vertici del cubo, il che implica che gli indici debbano essere o tutti dispari o tutti pari. Si possono generalizzare queste osservazioni dicendo che gli ordini [illegible] vrebbero essere relativamente deboli.

In effetti, questo è proprio ciò che si osserva. La figura a pag. 41 mostra uno dei primi gruppi di misure relative al cloruro di sodio e al cloruro di potassio fatte con lo spettrometro a ionizzazione, un apparato inventato da mio padre, W. H. Bragg, nel 1913. In ascisse sono riportate le misure dell'angolo di radenza, in ordinate le intensità della riflessione. I due picchi che si vedono in ciascun ordine sono le « righe » K_α e K_β dello spettro del palladio dell'anticatodo, la più intensa delle quali è la K_α. Gli ordini sono riflessi dalle facce del cristallo di indici cristallografici (100), (110) e (111). Come mostrano le curve, l'ordine (111) relativo al cloruro di sodio è piccolo in modo anomalo, mentre l'ordine (222) entra nella stessa sequenza degli ordini (200) e (220). Per il cloruro di potassio invece la capacità di diffusione degli atomi di potassio e di cloro è all'incirca identica, per cui l'ordine (111) è troppo debole per essere osservabile. È stato proprio sulla base di questi dati che venne confermata la disposizione strutturale di entrambi questi alogenuri alcalini. Anche se l'analisi precedente è alquanto semplificata, essa rappresenta un esempio tipico del metodo usato nelle prime determinazioni della struttura dei cristalli. Venivano misurati un certo numero di ordini di onde diffratte, con lo spettrometro a ionizzazione o con lastre fotografiche, e si cercava poi di trovare una disposizione atomica che rendesse conto delle intensità dei vari ordini.

-2-

sua determinazione è lo scopo finale di tutti i metodi sperimentali. Questa quantità è una misura, per ogni ordine (*hkl*), dell'intensità del fascio diffuso da una unità strutturale completa, espressa rispetto alla quantità diffusa da un singolo elettrone assunta come unità. Per esempio, la quantità $F(000)$ è diffusa in avanti con angolo zero, cosicché non vi è differenza di percorso che possa causare interferenze; $F(000)$ è perciò il numero totale di elettroni per unità strutturale. Per ordini più alti vi è una diminuzione d'intensità da attribuirsi all'interferenza.

È importante notare che $F(hkl)$ è un rapporto adimensionale, caratteristico soltanto della struttura cristallina e indipendente dalla lunghezza d'onda dei raggi X impiegati. Se si usa una lunghezza d'onda più breve, gli ordini compaiono ad angoli più piccoli e le differenze di percorso sono ridotte, ma le differenze di fase rimangono le stesse. Cioè $F(hkl)$ dipende soltanto dalla distribuzione della materia diffondente nella cella unitaria, il che è proprio l'obiettivo dell'analisi a raggi X.

Le basi teoriche per misurare i valori di $F(hkl)$ vennero formulate da C. G. Darwin in due brillanti articoli comparsi poco dopo la scoperta della diffrazione dei raggi X. A quei tempi le osservazioni sperimentali erano troppo approssimative per costituire un test per la sua teoria, e passò un certo numero di anni prima che si potesse applicarla.

Nei suoi primi calcoli Darwin fece l'ipotesi di un cristallo « idealmente perfetto ». I primi test approssimativi in-

Reciprocal lattice

real space

$$\vec{S}_{hkl} = h\vec{a}^* + k\vec{b}^* + l\vec{c}^* \qquad \vec{r} = u\vec{a} + v\vec{b} + w\vec{c}$$

$$\vec{a}^*\cdot\vec{b} = \vec{a}^*\cdot\vec{c} = \vec{b}^*\cdot\vec{c} = \vec{b}^*\cdot\vec{a} = \vec{c}^*\vec{a} = \vec{c}^*\cdot\vec{b} = 0$$

$$\vec{a}^*\cdot\vec{a} = \vec{b}^*\cdot\vec{b} = \vec{c}^*\cdot\vec{c} = 1$$

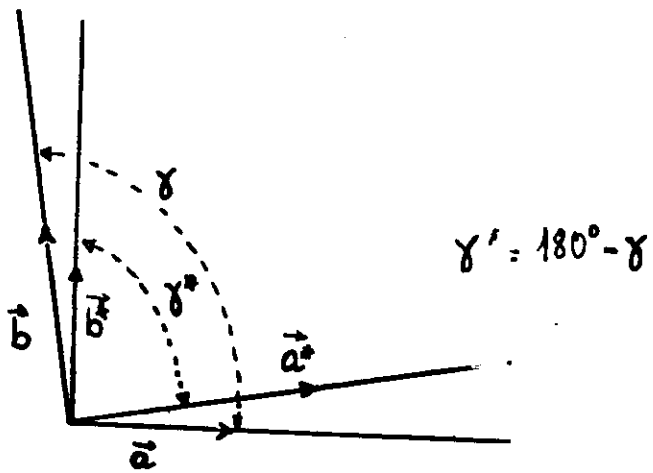

$$d_{hkl} = \frac{1}{|\vec{S}_{hkl}|} \qquad \text{where}$$

$$|\vec{S}_{hkl}|^2 = |h\vec{a}^* + k\vec{b}^* + l\vec{c}^*|^2 = h^2a^{*2} + k^2b^{*2} + l^2c^{*2} + 2hka^*b^*\cos\gamma^* + 2kl\,b^*c^*\cos\alpha^* + 2hl\,a^*c^*\cos\beta^*$$

for cubic unit cells:

$$d_{hkl} = \frac{1}{a^*(h^2+k^2+l^2)^{1/2}} = \frac{a}{(h^2+k^2+l^2)^{1/2}}$$

Crystal

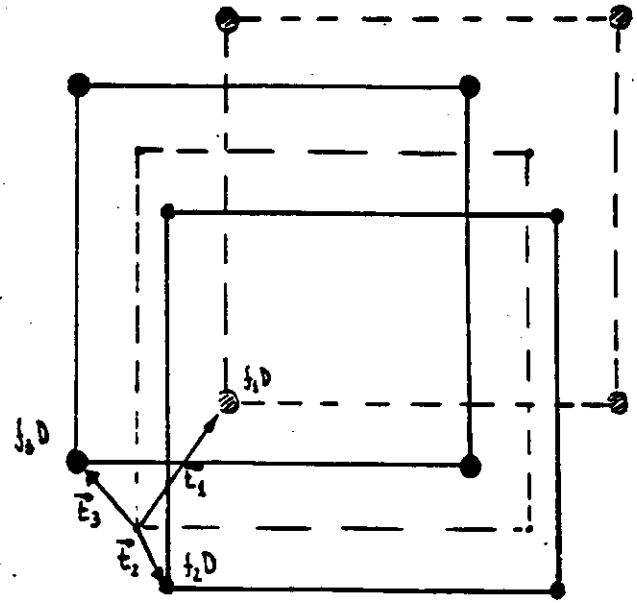

$$\vec{t}_i = x_i\vec{a} + y_i\vec{b} + z_i\vec{c}$$

$$A_i = \frac{A_i^0 e^{i\omega t}}{R} \sum_u^{N_1}\sum_v^{N_2}\sum_w^{N_3} e^{i2\pi\left\{[u\vec{a}+v\vec{b}+w\vec{c}]+\vec{t}_i\right\}\cdot\vec{S}} = \frac{e^{i\omega t}}{R} A_i^0 e^{i\vec{t}_i\cdot\vec{S}} \sum_u^{N_1}\sum_v^{N_2}\sum_w^{N_3} e^{i2\pi\vec{r}_{u,v,w}\cdot\vec{S}}$$

$$A = A_1 + A_2 + \dots + A_p = \frac{e^{i\omega t}}{R}\left(A_1^0 e^{i2\pi\vec{t}_1\cdot\vec{S}} + \dots + A_p^0 e^{i2\pi\vec{t}_p\cdot\vec{S}}\right) \sum_u^{N_1}\sum_v^{N_2}\sum_w^{N_3} e^{i2\pi\vec{r}_{u,v,w}\cdot\vec{S}}$$

$$A = \frac{e^{i\omega t}}{R}\left(\sum_i^P A_i^0 e^{i2\pi\vec{t}_i\cdot\vec{S}}\right) \sum_u^{N_1}\sum_v^{N_2}\sum_w^{N_3} e^{i2\pi\vec{r}_{u,v,w}\cdot\vec{S}}$$

when $N_1, N_2, N_3 \longrightarrow \infty$

$$A_{hkl} = \frac{e^{i\omega t}}{R}\left(N_1^2 N_2^2 N_3^2\right) \sum_i^P A_i^0 e^{i2\pi\vec{S}\cdot\vec{t}_i}$$

since $\vec{S}\cdot\vec{t}_i = (h\vec{a}^* + k\vec{b}^* + l\vec{c}^*)(x_i\vec{a} + y_i\vec{b} + z_i\vec{c}) = hx_i + ky_i + lz_i$

$$A_{hkl} = K\sum_i^P f_i e^{i2\pi(hx_i + ky_i + lz_i)} \qquad \text{if } A_i^0 = f_i D$$

$$F_{hkl} = \sum_i^P f_i e^{i2\pi(hx_i + ky_i + lz_i)}$$

$$\rho(x,y,z) = \frac{1}{V_{cell}} \sum_h \sum_k \sum_{l=-\infty}^{+\infty} F_{hkl}\, e^{-2\pi i (hx+ky+lz)}$$

$$\rho(x,y,z) = \frac{2}{V_{cell}} \sum_h \sum_k \sum_{l=0}^{\infty} |F_{hkl}| \cos\left\{2\pi\left(hx+ky+lz + \frac{\varphi}{2\pi}\right)\right\}$$

phase

PHASE PROBLEM

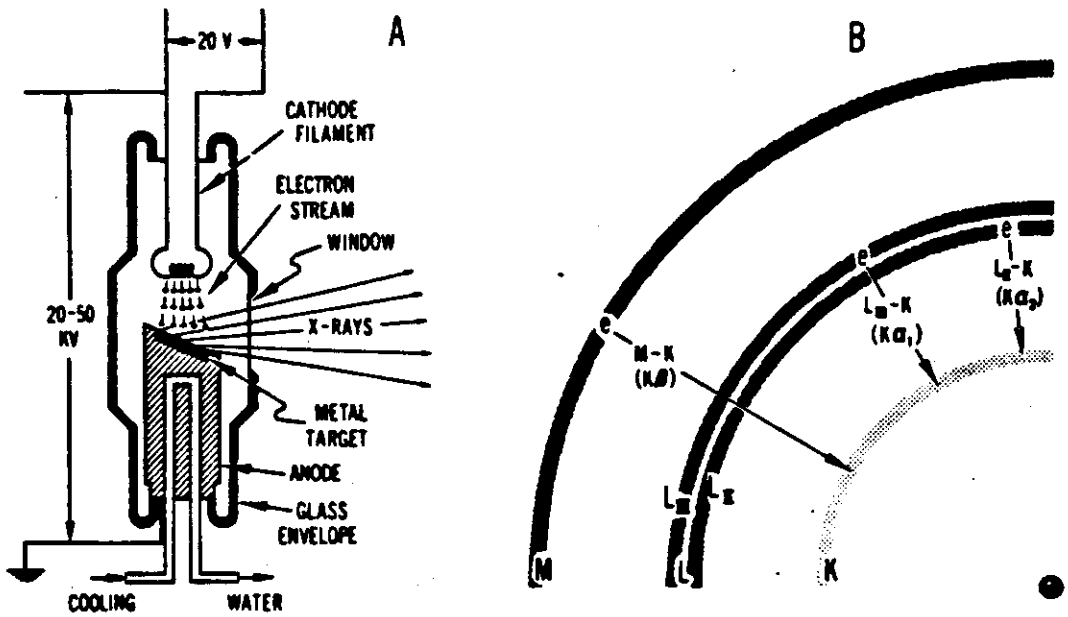

FIGURE 13–1

(A) Generalized cross section through an X-ray tube. High-energy electrons from the cathode strike the metal target on the anode, exciting the metal atoms by "knocking" electrons out of their K shells.

(B) Schematic energy-level diagram illustrating how the excited K shell captures electrons from outer shells, the M–K transition producing $K\beta$ X-rays, the L–K transitions producing $K\alpha_1$ and $K\alpha_2$ X-rays.

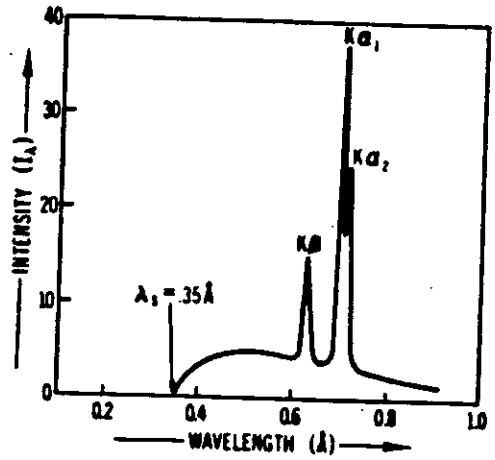

FIGURE 13-2

Relative intensities I_λ for the various wavelengths of X-rays emitted by an X-ray tube with a molybdenum target operated at 35 kV.

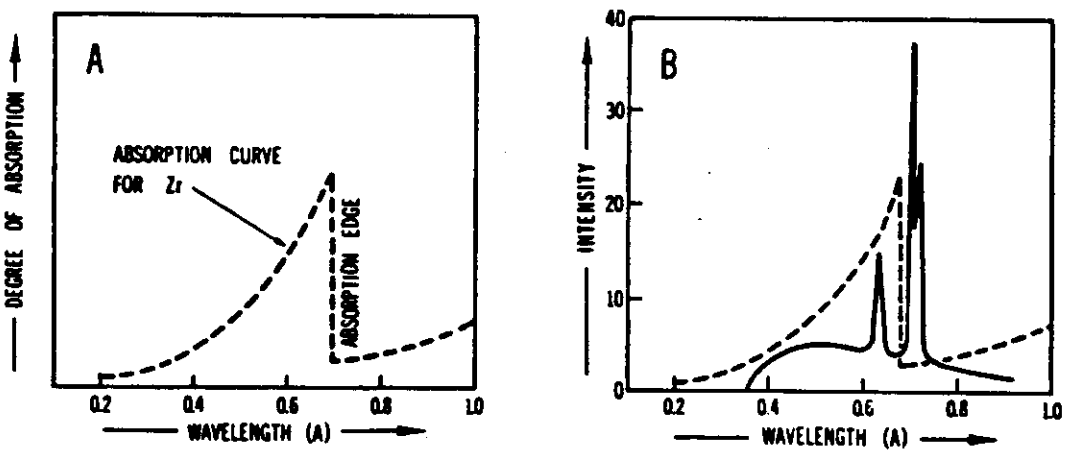

FIGURE 13-3

(A) Absorption curve for zirconium foil for X-rays of wavelengths between 0.2 and 1.0 Å. The abrupt decrease in ability to absorb at $\lambda = 0.687$ Å marks zirconium's *absorption edge*.

(B) Curve showing the intensities of X-rays emitted by a molybdenum tube operated at 35 kV on which is superimposed the absorption curve for zirconium foil. The absorption edge for zirconium (atomic number, 40) falls between the $K\beta$ and $K\alpha$ peaks for molybdenum (atomic number, 42). This permits zirconium foil to filter out the Mo$K\beta$ radiation from the X-rays emitted by a molybdenum tube.

contains many thousands of small, randomly oriented crystals, and consequently many grains are expected to be in the proper position at all times to permit diffraction from all the permissible lattice planes.

Figure 1*a* illustrates a single grain in a powder sample which has a lattice layer oriented perpendicular to the page of the book and is inclined to the incident x-ray beam at the appropriate diffraction angle θ. The diffracted beam, still in the plane of the paper, is inclined to the lattice layer by the same angle θ and to the direct beam by angle 2θ. Since there are many thousands of grains in the powder sample, several of them will be in a position such that they have the same lattice layer inclined to the

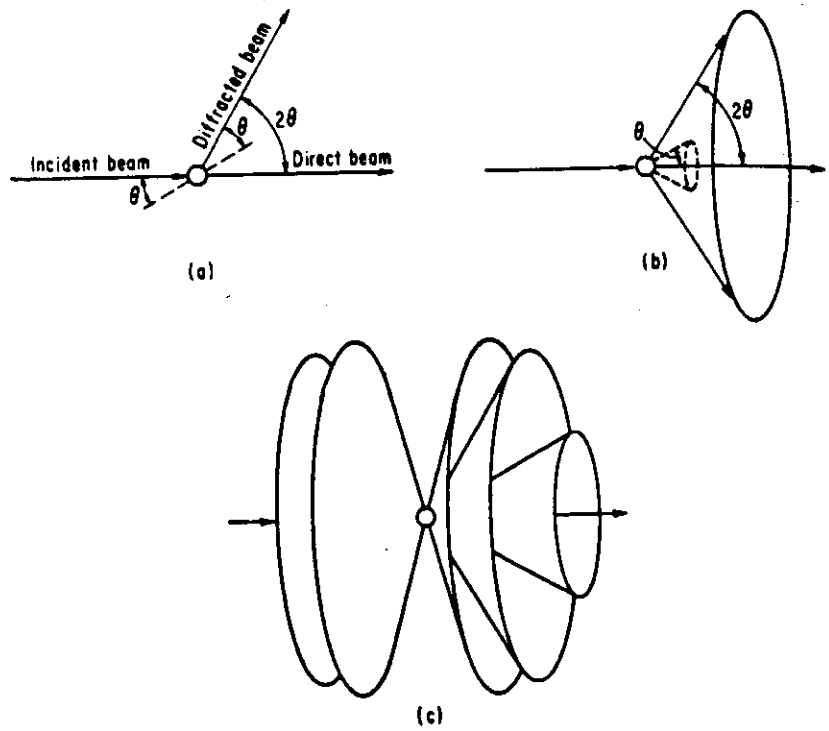

FIG. 1. Illustration of the diffraction of x-rays (a) by a lattice layer of a single grain, (b) by identical lattice layers from many grains, and (c) by different lattice layers of many grains.

incident beam by the same angle θ of Fig. 1*a*, and since the Bragg equation defines the inclination of the lattice plane in one dimension only, there will be identical lattice layers in the proper diffraction position oriented tangentially along the surface of a cone whose inclination with the direct beam will be θ. Similarly there will be a cone of diffracted beams inclined to the direct beam by an angle of 2θ (see Fig. 1*b*). Simultaneously, other lattice layers with different interplanar spacing and, consequently, with different θ inclination will be in diffracting position, thus giving rise to various diffraction cones. Several diffraction cones are illustrated in Fig. 1*c*.

All the powder cameras are designed to record these diffraction cones; however, many of them differ in the geometry and construction of the design. There are three major types of powder cameras: (1) the Debye-Scherrer camera, (2) the focusing cameras, and (3) the flat-film cameras. These three cameras select different ranges of the diffraction spectrum, record the diffraction cones in different ways, and emphasize

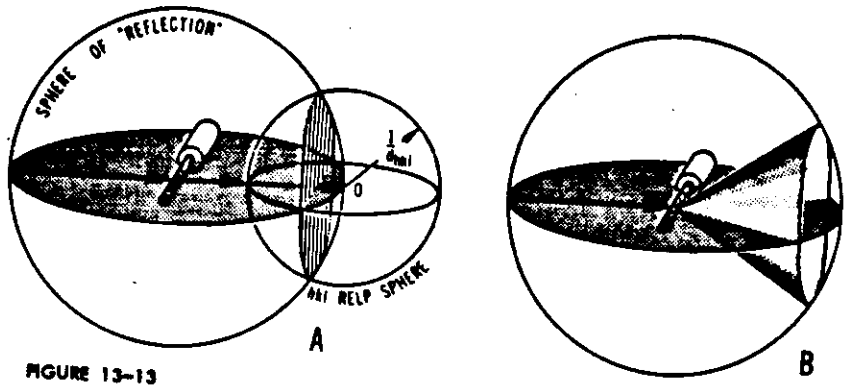

FIGURE 13-13

(A) Where a powder rod is struck by the direct beam, we locate the center of the imaginary sphere of reflection (radius, $1/\lambda$). The origin of the reciprocal lattice for each of the variously oriented grains in the powder rod is at O, the point where the direct beam emerges from this sphere of reflection. If the same hkl relp were plotted, for example, relp 213, for each of these variously oriented grains, a relp sphere would result of radius $1/d_{hkl}$, that is, of radius $1/d_{213}$ for our specific example. This relp sphere intersects the sphere of reflection in the dotted circle (vertically ruled). (B) From the powder rod, diffracted rays travel toward those relps located on the dotted circle to form the cone shown. Numerous other relp spheres, each with a different radius, for example, $1/d_{100}$, $1/d_{111}$, $1/d_{221}$, could be drawn centered at O and would similarly intersect the sphere of reflection in circles to which cones of diffracted rays would proceed from the powder rod.

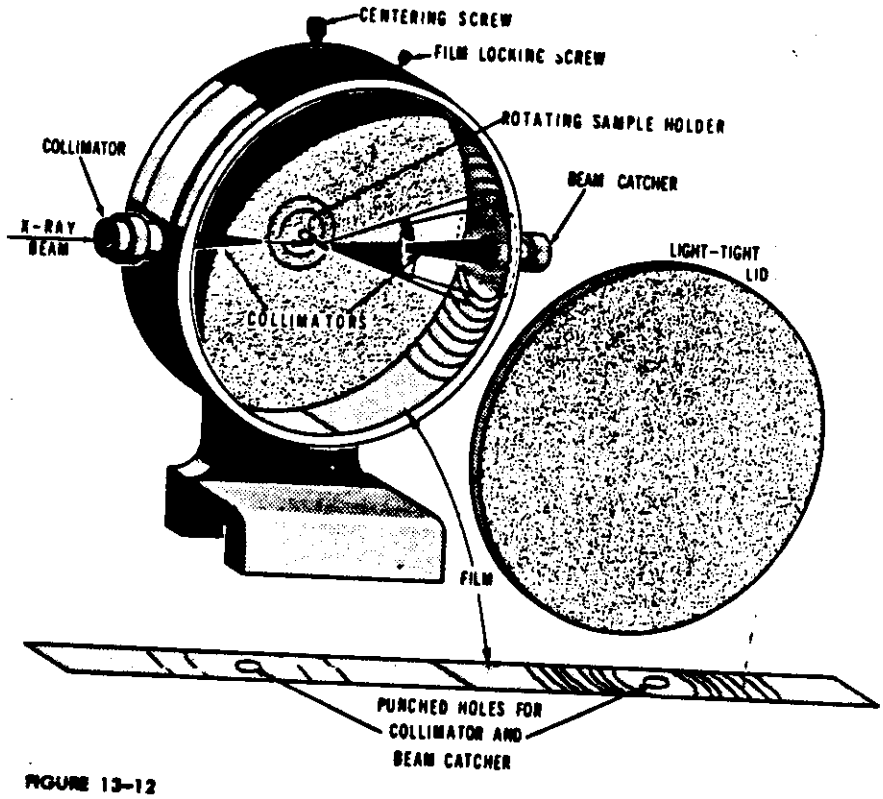

FIGURE 13-12

Schematic view of a powder camera with its light-tight lid removed. Its collimator is placed against the exit port of the X-ray tube and blocks out all X-rays except a fine beam that impinges on the powder rod. This powder rod is rotated about its axis by a small motor which is not shown. For reasons to be discussed in Figure 13-13, cones of diffracted X-rays emanate from the powder rod where it is struck by the direct beam, these cones exposing the film in a series of arcs which, after the film is developed, might appear as shown here.

12

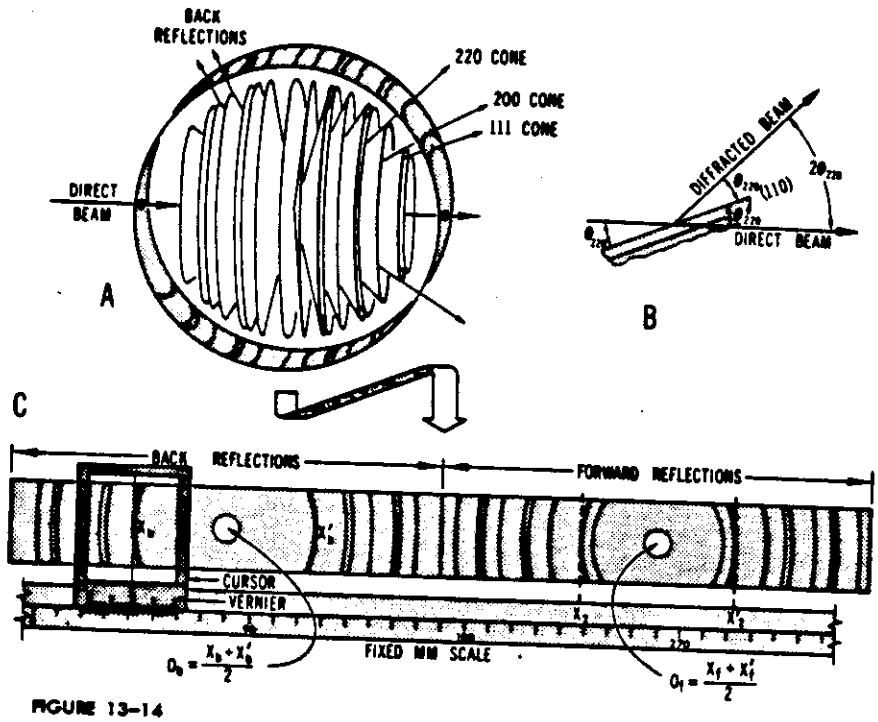

FIGURE 13–14

(A) The numerous cones of diffracted rays that emanate from a powder rod (hidden by the cones) expose the film strip in a powder camera to produce a series of arcs. The powder camera itself is not shown. The powder rod would be rotating on its axis, which is also the axis of the squat cylinder formed by the film strip. (B) Cross section (enlarged 100,000,000X) of a grain whose diffracted beam lies along the arrow on the 220 cone in (A). As this cross section is rotated 360° around the direct beam as an axis, it successively represents the cross section of each grain in the rod that produces a diffracted ray lying in the 220 cone. If we compare this cross section with itself after a 180° rotation around the direct beam, we see that 4θ represents the cone angle, that is, the angle between the two most divergent rays in the same diffraction cone.

(C) Enlarged drawing of the film in (A) after its processing and mounting onto a device for measuring the distance between arcs on a powder film. For example, the cursor now indicates the midpoint of arc x_b to be above 40.6 on the fixed millimeter scale (whose finer divisions have been largely omitted). The cursor could next be slid to coincide with the midpoint of x_b'. The distance in millimeters between x_b and x_b', corrected for film shrinkage, equals 4θ for the cone which produced these arcs, *if a powder camera was used whose circumference equals 360 mm.* Similarly, we could determine 4θ for arcs resultant from forward reflections, for example, the distance between x_2 and x_2'. Note that O_b, the arithmetric average of two arcs from the same back-reflected diffraction cone $[\frac{1}{2}(x_b + x_b')]$ marks the point where the direct beam enters the film in (A). Similarly O_f, the arithmetric average of two arcs from the same forward-reflected cone, is the coordinate of the point where the direct beam leaves the powder camera (through a hole punched in the film). The intensities of the back reflections are greatly exaggerated.

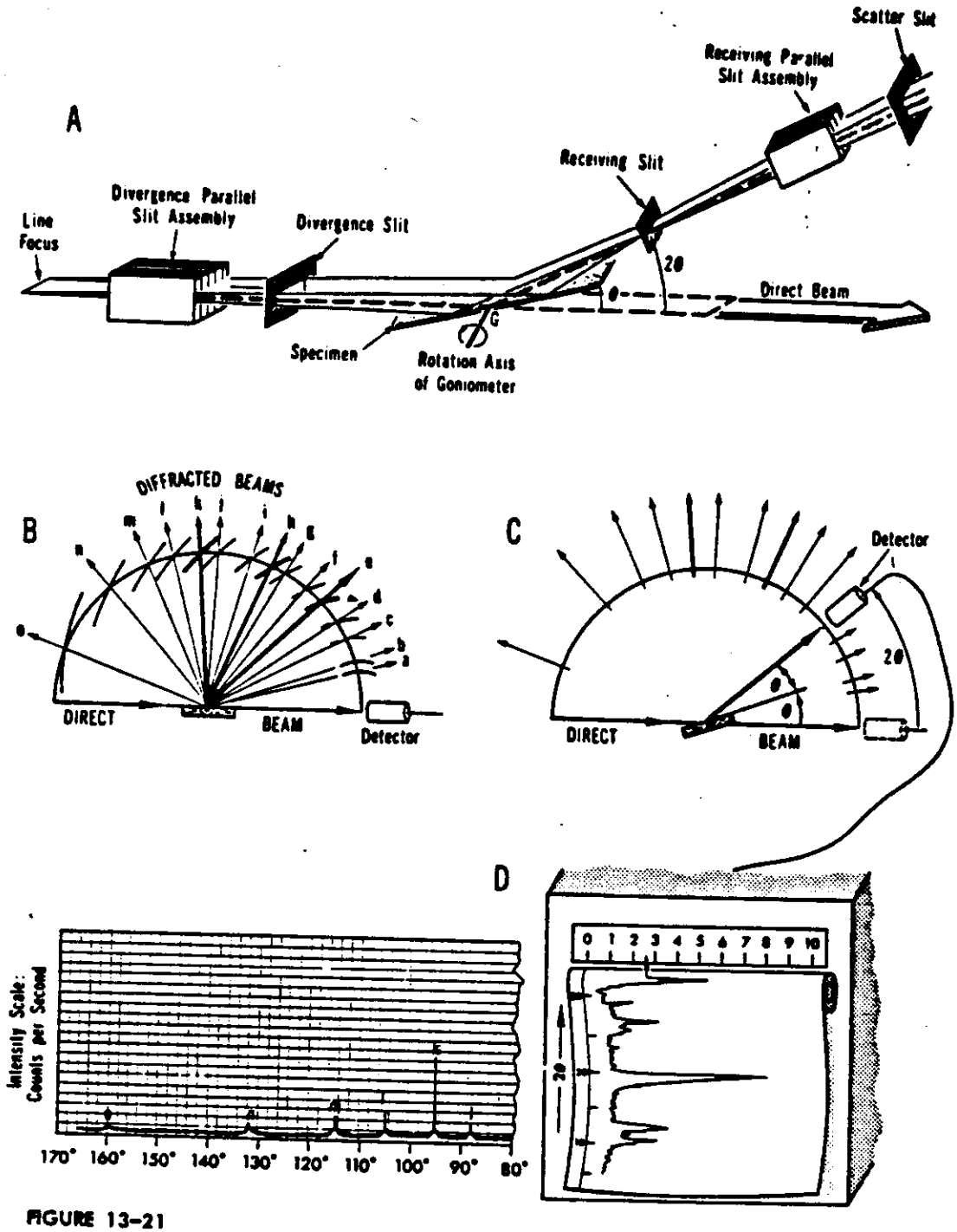

FIGURE 13–21

(A) Schematic drawing of the principal parts of an x-ray diffractometer. X-rays from the tube's line focus are collimated by passage through a parallel slit assembly (Soller slit) and a divergence slit before striking the powder (stippled) on a glass slide or sample holder. While the slide (length exaggerated) rotates about axis G so as to be at an angle θ to the direct beam, a detector (stripped of its housing to reveal its receiving, Soller, and scatter slits) scans through the angle 2θ.
(B) Segments of relp spheres a, b, ... m, n, o for the crystalline powder intersect the sphere of reflection (semicircle) to produce diffracted rays a, b, ... m, n, o.
(C) While the sample rotates through an angle θ about the axis G, which is now

$$d^2_{hkl} = \frac{a^2}{(h^2+k^2+\ell^2)} \qquad \left(\frac{d_1}{d_{hkl}}\right)^2 = \frac{h^2+k^2+\ell^2}{h_1^2+k_1^2+\ell^2}$$

	N
100, 010, 001	1
110, 011, 101	2
111	3

TABLE 13–5

Observed 2θ and Calculated d_1^2/d^2 Values for a Powder Film of Synthetic Spinel, $MgAl_2O_4$

$2\theta_{obs}$	d_{hkl}	d^2_{hkl}	d_1^2/d^2	hkl	N[a]	a_{calc}[b]
19.02α	4.6658	21.7697	1	111	3	8.0814
31.30α	2.8577	8.1664	2.666	220	8	8.0828
36.894α	2.4365	5.9365	3.667	311	11	8.0810
44.84α	2.0212	4.0852	5.329	400	16	8.0848
55.702α	1.6501	2.7232	7.994	422	24	8.0838
59.427α	1.5553	2.4190	8.999	511/333	27	8.0816
65.287α	1.4291	2.0423	10.659	440	32	8.0842
68.736α	1.3656	1.8649	11.673	531	35	8.0790
74.19α	1.2781	1.6335	13.327	620	40	8.0834
77.388α	1.2331	1.5205	14.317	533	43	8.0860
82.691α	1.1670	1.3619	15.984	444	48	8.0852
85.78α	1.1327	1.2830	16.968	711/551	51	8.0891
94.171α_1	1.0517	1.1063	19.678	731/553	59	8.0783
94.451α_2	1.0520					8.0806
99.37α_1	1.0102	1.0203	21.337	800	64	8.0816
99.72α_2	1.0101					8.0808
107.92α_1	0.95257	0.90729	23.994	822/660	72	8.0828
108.327α_2	0.95248					8.0821
111.26α_1	0.93318	0.87094	24.995	751/555	75	8.0816
111.656α_2	0.93330					8.0826
116.944α_1	0.90365	0.81640	26.665	840	80	8.0825
117.45α_2	0.90345					8.0807
120.50α_1	0.88719	0.78582	27.667	911/753	83	8.0827
121.074α_2	0.88686					8.0797
130.744α_1	0.84733	0.71797	30.321	931	91	8.0836
131.366α_2	0.84734					8.0831
138.028α_1	0.82497	0.68056	31.987	844	96	8.0830
138.785α_2	0.82495					8.0828

[a] $N = h^2 + k^2 + l^2$

[b] $a = d\sqrt{N}$

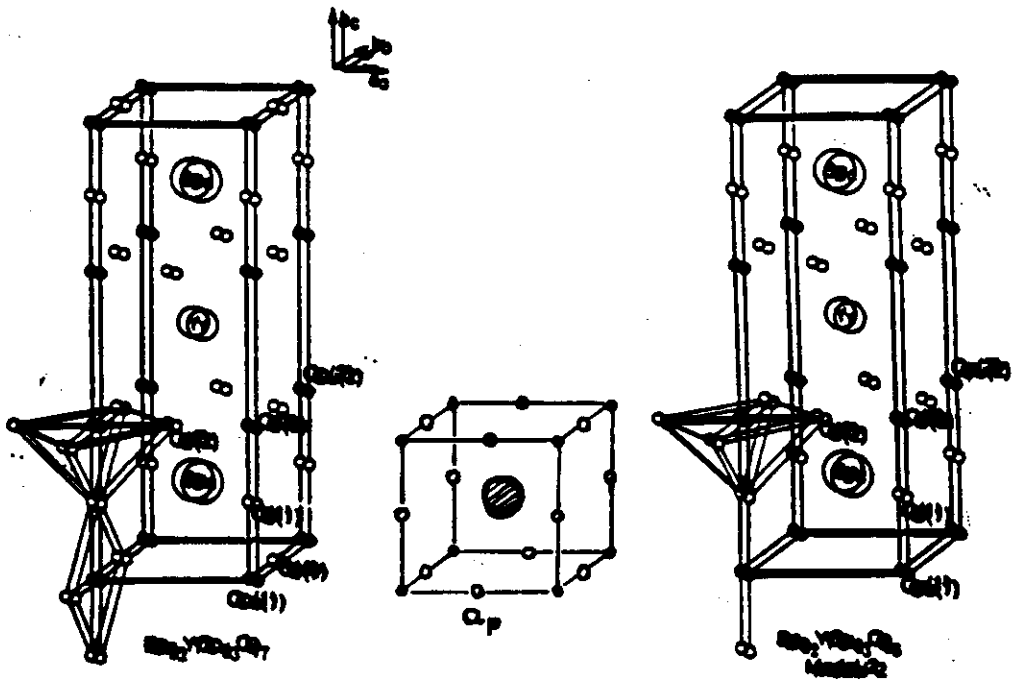

Fig. 4
Schematic unit cells for $Ba_2YCu_3O_x$.

$a \cong b \cong a_p$

$c \cong 3 a_p$

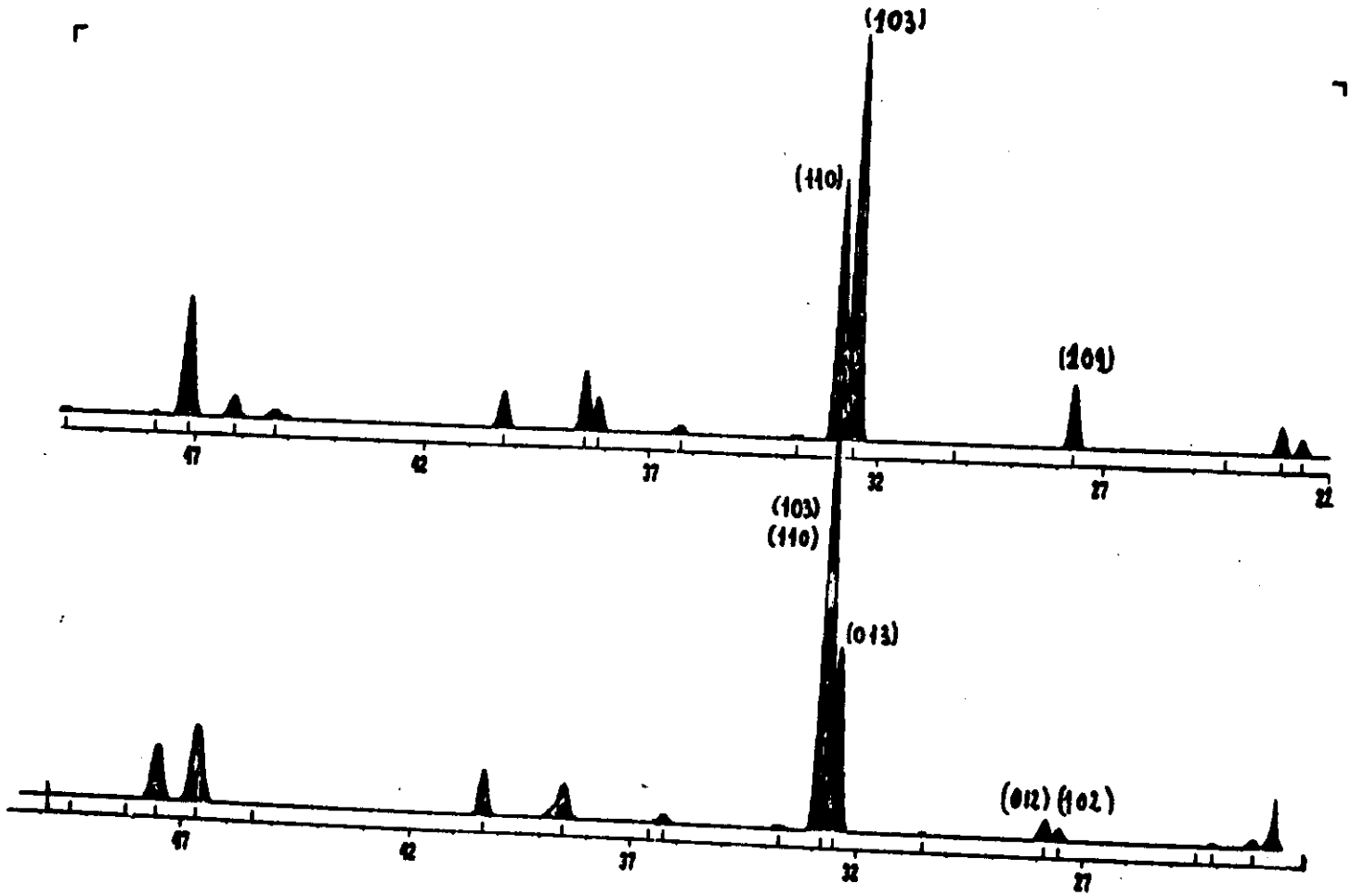

a = b = 3.86 Å
c = 11.80 Å

a = 3.82 Å
b = 3.88 Å
c = 11.68 Å

29

I

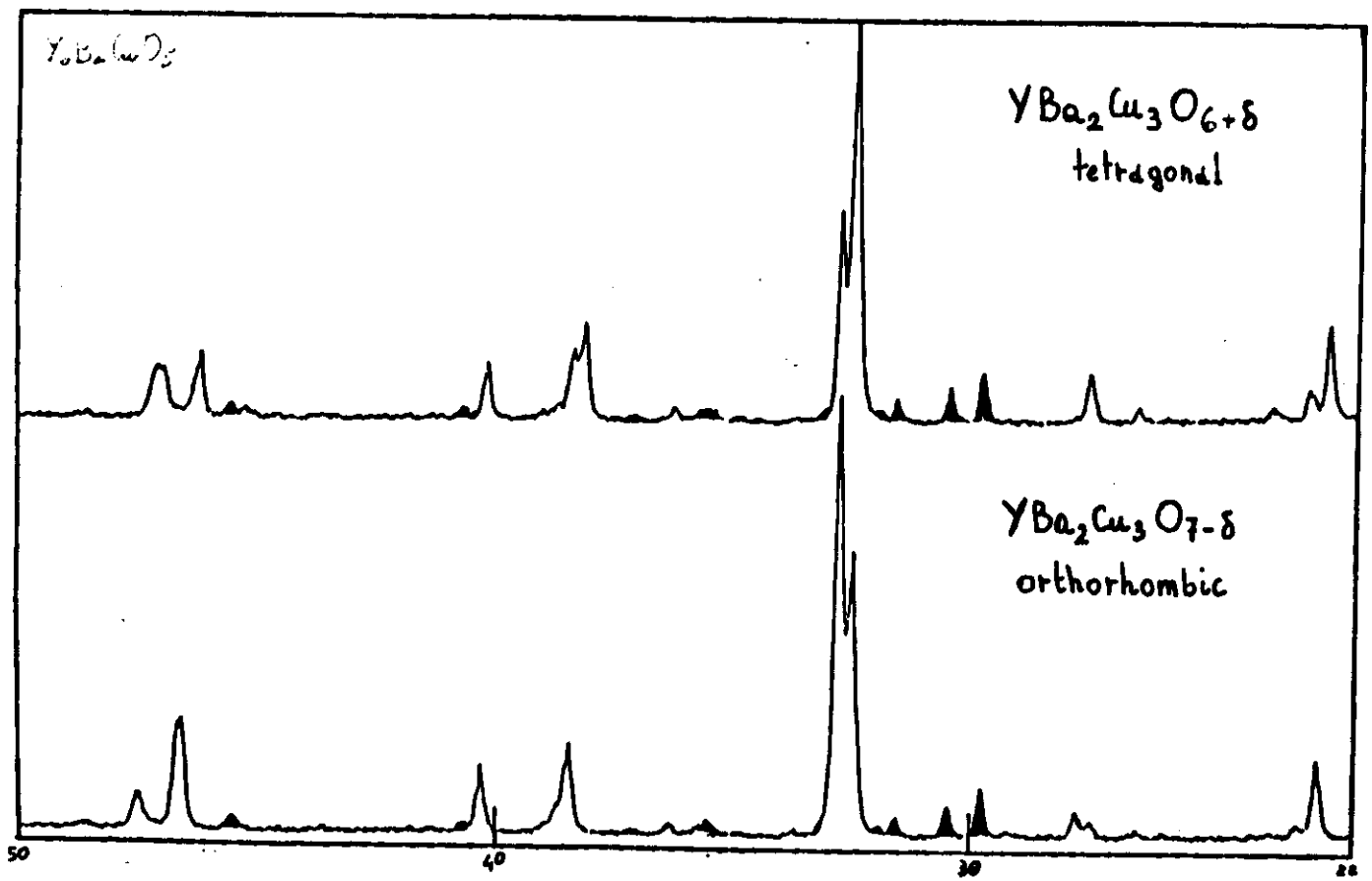
$YBa_2Cu_3O_{6+\delta}$
tetragonal
$YBa_2Cu_3O_{7-\delta}$
orthorhombic
50
40
30
2θ

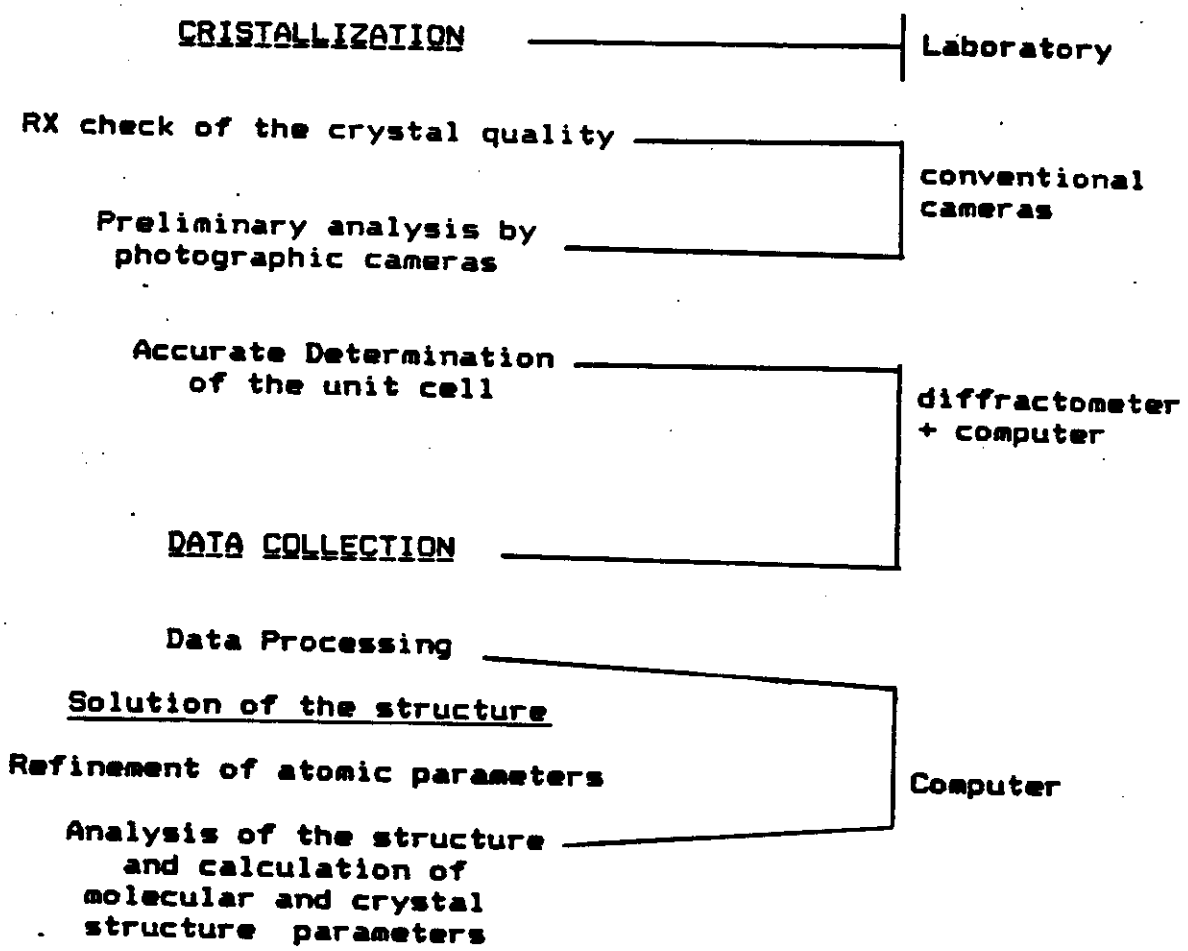
CRISTALLIZATION
Laboratory
RX check of the crystal quality
conventional cameras
Preliminary analysis by photographic cameras
Accurate Determination of the unit cell
diffractometer + computer
DATA COLLECTION
Data Processing
Solution of the structure
Refinement of atomic parameters
Computer
Analysis of the structure and calculation of molecular and crystal structure parameters

CAD-4

Goniometer

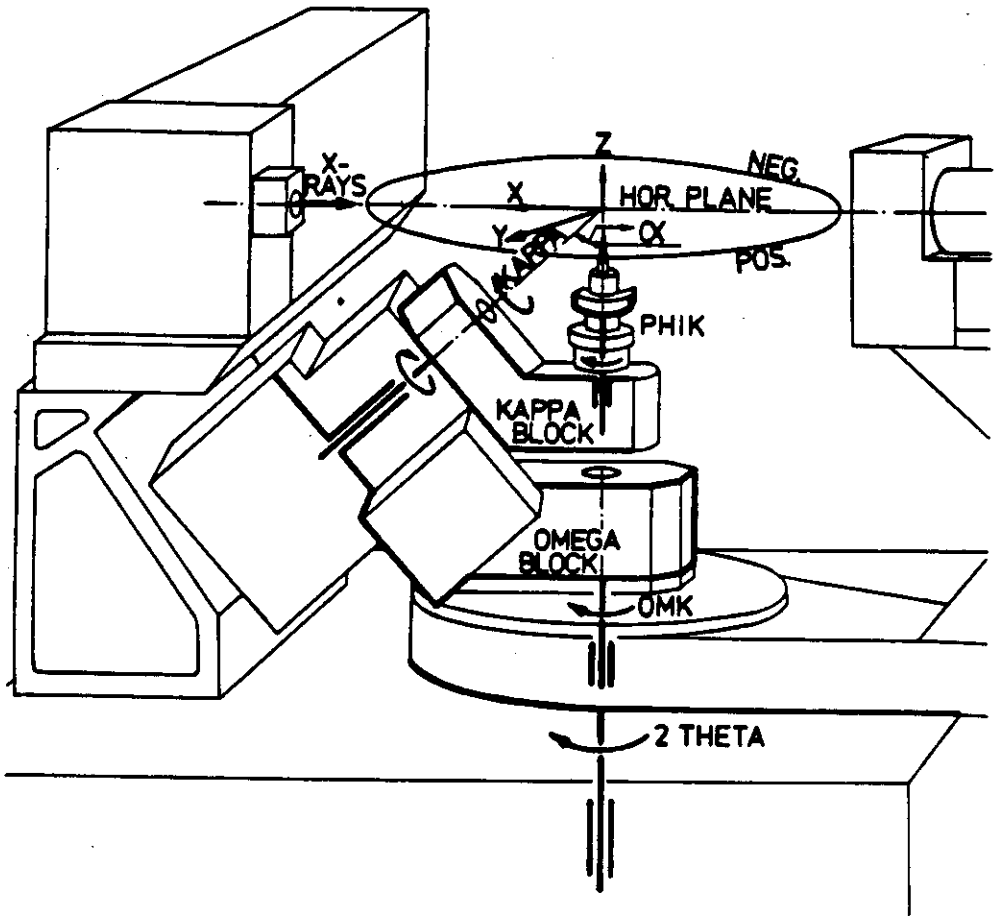

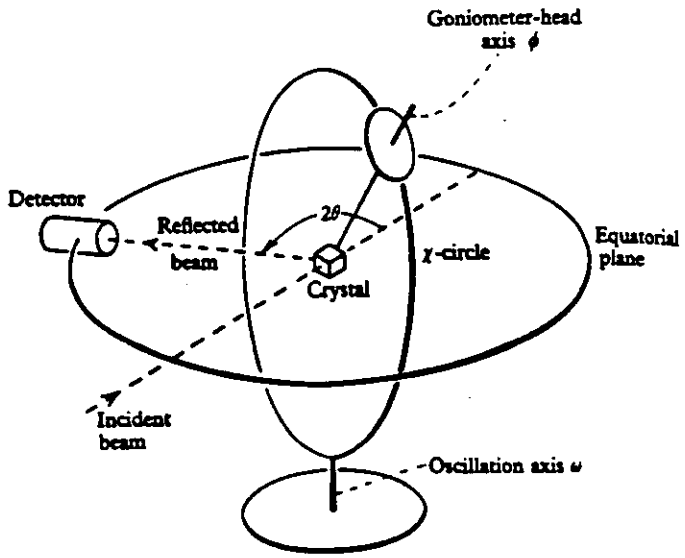

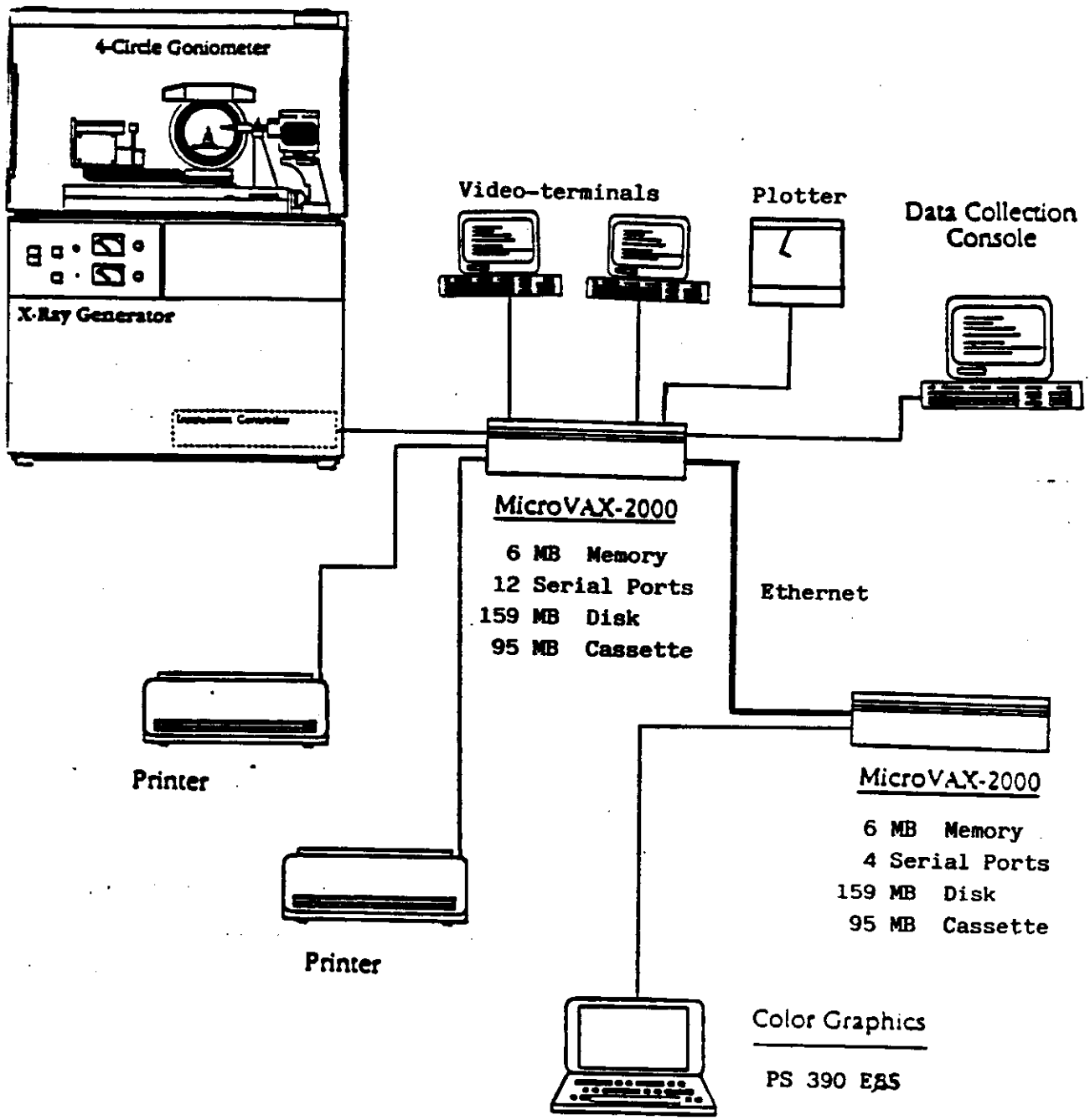
4-Circle Goniometer
X-Ray Generator
Video-terminals
Plotter
Data Collection Console
MicroVAX-2000
6 MB Memory
12 Serial Ports
159 MB Disk
95 MB Cassette
Ethernet
Printer
Printer
MicroVAX-2000
6 MB Memory
4 Serial Ports
159 MB Disk
95 MB Cassette
Color Graphics
PS 390 E&S

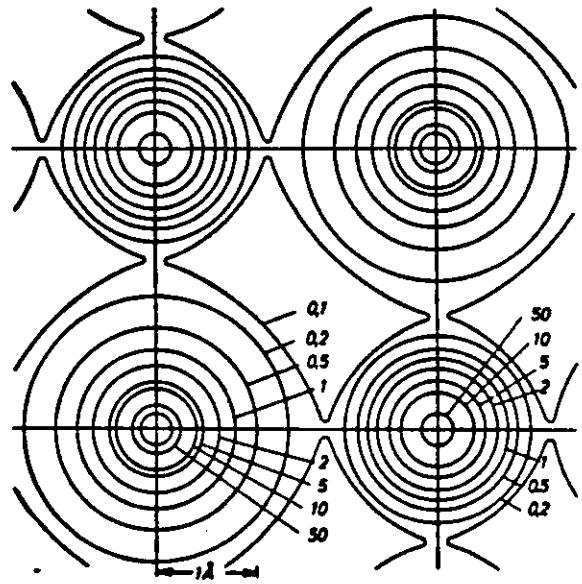

FIG. 331. A section through the electron density in the plane $x=0$ for sodium chloride

Collection of the XR pattern

Powder methods

1. Determination of the unit cell
2. Refinement of "simple" crystal structures (Rietveld method)
3. Crystallite size, etc.

Intensity is collected as function of ϑ. Thus diffracted beams with equal or very close ϑ overlap.

Single crystal methods

1. Determination of the unit cell
2. Solution of the crystal structure
3. Refinement of the crystal structure

Intensity of each diffracted beam is measured without overlap.

Nobel Prizes for Studies Involving X-ray Diffraction and Crystallography

Physics		
1914	Max von Laue	Discovery of diffraction of X-rays by crystals
1915	Sir William H. Bragg, William L. Bragg	Research on crystal structures using X-rays
1937	Clinton J. Davisson, Sir George P. Thompson	Electron diffraction of crystals
Chemistry		
1936	Peter J. Debye	Contribution toward understanding molecular structure through work on the dipole moment and the X-ray and electron diffraction in gases
1954	Linus C. Pauling	Research on the chemical bond and structural clarification of complex substances
1962	Max F. Perutz, John C. Kendrew	Structural determination of myoglobin and hemoglobin using X-ray diffraction
1964	Dorothy Crowfoot Hodgkin	Structural clarification of important biochemical substances using X-ray analysis
1976	William N. Lipscomb	Work on the structures of boron hydrides
1982	Aaron Klug	Structure of nucleic acid–protein complexes
1985	Herbert A. Hauptman, Jerome Karle	Direct methods in crystal structure determination
Physiology and Medicine		
1962	James D. Watson, Francis H. C. Crick, Maurice H. F. Wilkins	Discovery of the molecular structure of nucleic acids and its significance for the genetic code
1988	R. HUBER J. DEISENHOFER H. MICHEL	MOLECULAR STRUCTURAL OF THE PHOTOSYNTHETIC REACTION CENTER.

Resource List

Listed below are some of the books that are useful in teaching crystallography. This list is by no means comprehensive. Most of the books and materials necessary to teach crystallography can be purchased from the Polycrystal Book Service, P.O. Box 3439, Dayton, OH 45401.

Teaching Pamphlets

International Tables for Crystallography: Brief Teaching Edition of Volume A Space-Group Symmetry: Hahn, T., Ed.; Reidel: 1985.

IUCr Commission on Crystallographic Teaching. Booklets on various aspects of crystallography. Taylor, C.A., Ed.; 19 pamphlets, 1981–1984.

Crystals and Crystal Growth

Evans, R. C. *An Introduction to Crystal Chemistry*; Cambridge University: New York, 1964.

Holden, A.; Singer, P. *Crystals & Crystal Growing*; Doubleday: New York, 1960.

Holden, A.; Morrison, P. *Crystals and Crystal Growing*; MIT Press: Cambridge, MA, repr. 1982.

McPherson, A. *Preparation & Analysis of Protein Crystals*; Wiley: New York, 1982.

Nye, J. F. *Physical Properties of Crystals: Their Representation*; Oxford University: New York, 1957.

Wood, E. A. *Crystals and Light*; Van Nostrand: New York, 1977.

Wood, E. A. *Crystals: A Handbook for School Teachers*; 1972.

X-Ray Diffraction and Crystal Structure Analysis

Blundell, T. L.; Johnson, L. *Protein Crystallography*; Academic: New York, 1976.

• Buerger, M. J. *Crystal Structure Analysis*; Krieger: Melbourne, FL, repr 1980.

• Buerger, M. J. *X-ray Crystallography*; Krieger: Melbourne, FL, repr 1980.

Burns, C. W. *Chemical Crystallography*; Clarendon: New York, 1961.

Cullity, B. D. *Elements of X-ray Diffraction*; Addison–Wesley: Reading, MA, 1978.

Curtin, D. Y. *Introduction to Crystallography*; software on two disks for Apple II, Franklin, and Bell & Howell Computers (Geom. Cryst.), 1984.

Dunitz, J. *X-ray Analysis and the Structure of Organic Molecules*; Cornell University: Ithaca, NY, 1979.

Glusker, J. P.; Trueblood, K. N. *Crystal Structure Analysis: A Primer*; Oxford University: New York, 1985.

Holmes, K. C.; Blow, D. M. *The Use of X-ray Diffraction in the Study of Protein and Nucleic Acid Structure*; Krieger: Melbourne, FL, repr 1979.

• Klug, H.; Alexander, L. E. *X-ray Diffraction Procedures*, 2nd ed.; Wiley-Interscience: New York, 1974.

Ladd, M. F. C.; Palmer, R. A. *Structure Determination by X-ray Crystallography*; Plenum: New York, 1985.

• Lipson, H.; Cochran, W. *Determination of Crystal Structures*, rev. ed.; Cornell University: Ithaca, NY, 1966.

Phillips, F. C. *An Introduction to Crystallography*; 3rd ed.; Longmans, Green: New York, 1963.

• R. W. JAMES, The Optical Principles of the Diffraction of X-Rays G. Bell & Sons Ltd., London, 1967

• Stout, G. H.; Jensen, L. *X-ray Structure Determination. A Practical Guide*; Macmillan: New York, 1972.

Woolfson, M. M. *An Introduction to X-ray Crystallography*; Cambridge University: New York, 1970.

Methods in Enzymology; Wyckoff, W. H.; Hirs, C. H. W.; Timasheff, S. N., Eds.; Academic: New York, 1985; Vol. 114, Part A, Vol. 115, Part B.

International Tables for Crystallography, Volume A, 1–4; Hahn, T., Ed.; Reidel: 1983.

Symmetry

Bernal, I.; Hamilton, W. H.; Ricci, J. S. *Symmetry: A Stereoscopic Guide for Chemists*; W. H. Freeman: New York, 1972.

Hargittai, I. *Symmetry—Unifying Human Understanding*; Pergamon: New York, 1986.

Holden, A. *Shapes, Space & Symmetry*; Columbia University: New York, 1971.

MacGillavry, C. H. *Symmetry Aspects of Escher's Periodic Drawings*, 2nd ed.; Bohn, Scheltema & Holkema: Utrecht, 1976.

Aspects of Symmetry; International Film Bureau Inc., 332 South Michigan Avenue, Chicago, IL 60604.

Symmetry; International Film Bureau Inc., 332 South Michigan Avenue, Chicago, IL 60604.

Results of Crystal Structure

Beevers Miniature Models Unit, Department of Chemistry, University of Edinburgh, West Mains Road, Edinburgh EH9 3JJ, United Kingdom.

Dickerson, R. E.; Geis, I. *Structure & Action of Proteins*; Benjamin/Cummings: Menlo Park, CA, 1969.

Donohue, J. *The Structures of the Elements*; Krieger: Melbourne, FL, repr 1982.

Glusker, J. P. *Structural Crystallography in Chemistry and Biology*; Hutchinson Ross: 1981.

• Wells, A. F. *Structural Inorganic Chemistry*, 5th ed.; Oxford University: New York, 1984, repr w/corr 1986.

Wyckoff, R. W. G. *Structure of Crystals*; Krieger: Melbourne, FL, 1935, repr 1963.

Books of General Interest

Bragg, W. H. *X-rays and Crystal Structure*, 2nd ed.; Bell, 1924.

Bragg, W. H. *Introduction to Crystal Analysis*; Bell, 1928.

Ewald, P. P. *Fifty Years of X-ray Diffraction*; N. V. A. Oosthoek's Uitgeversmaatschappij, 1962.

Sayre, A. *Rosalind Franklin & DNA*; Norton: New York, 1978.

Watson, J. D. *The Double Helix*; Atheneum: New York, repr 1980.

Data Bases

Cambridge Crystallographic Data Base; National Technical Information Service (NTIS), U.S. Department of Commerce, 5285 Port Royal Road, Springfield, VA 22161.

Protein Data Bank; Chemistry Department, Brookhaven National Laboratory, Upton, NY 11973.

Inorganic Crystal Structure Data Base; contact Paul Dellevigne, 7 Woodland Avenue, Larchmont, NY 10538.